Computer Assisted Mechanics and Engineering Sciences, 9: 373–390, 2002.

Advanced modelling of flexible multibody systems using virtual bodies[1]

João Gonçalves and Jorge Ambrósio
Instituto de Engenharia Mecânica (IDMEC), Instituto Superior Técnico
Av. Rovisco Pais, 1041-001 Lisboa, Portugal

(Received August 8, 2000)

When new formulations for the description of flexible multibody systems are proposed, often they imply the use of new sets of generalized coordinates, even if the finite element method is used to describe the system flexibility. The adoption of such formulations implies that an additional effort must be made to describe the kinematic constraints that involve flexible bodies. The commercial multibody codes generally have good kinematic joint libraries for rigid bodies, but they are limited in the type of joints available in what flexible bodies are concerned. This work proposes and demonstrates that such limitations can be overcome by using virtual rigid bodies. The idea is to develop a single kinematic joint that restricts all relative degrees of freedom between one or more nodes of the flexible body and a rigid body. The designation of virtual body derives from assuming that it is a massless rigid body. In this form any of the kinematic joints between rigid bodies available in the multibody code libraries, can be used. In the process it is shown that the interaction of the user with the multibody code is much simpler. The numerical problems resulting from ill-conditioned mass matrix, due to the null inertias of the virtual bodies, are avoided by using a sparse matrix solver for the solution of the equations of motion. The proposed formulation is applied to a complex flexible multibody system, represented by the model of a road vehicle with flexible chassis, the results are presented and the discussion on the relative virtues and drawbacks of the current methodologies is made with emphasis on the models and algorithms used.

1. Introduction

The need to use complex computer models of flexible systems requires a highly accurate and efficient development of computer tools. New formulations have been proposed using sets of generalized deformation coordinates to describe the system flexibility. Ambrósio and Gonçalves [2] have proposed a linear deformation methodology for flexible bodies, where a flexible body is split into a rigid part and a flexible part. The system mass matrix is derived based in a lumped mass formulation from finite element methods and all node coordinates are expressed with reference to a inertial frame. With these assumptions it is possible to obtain a constant and lumped mass matrix for the flexible body, with all the terms involved obtained directly from standard finite element codes. The inertia coupling terms obtained are independent of the shape function used to describe the finite elements and the coupling of the linear elastodynamics of the flexible body with the gross rigid body motion is full preserved.

As all new formulations, this also requires the derivation of kinematic constraints for several joint types. Most of the multibody codes, either commercial or for research purpose, already have good libraries of kinematic joints between rigid bodies. However when flexible bodies are involved, the effort on deriving all those joints must be duplicated. Moreover, such effort is aggravated due to the complexity of dealing with nodal deformations and rotations. That represents a heavy workload and is prone to code errors. A form of avoiding these difficulties is by using virtual rigid bodies, has proposed by Bae et al. [5]. The use of virtual rigid bodies associated with joints with flexible

[1]This is an extended version of the article presented at the NATO Advanced Research Workshop on the *Computational Aspects of Nonlinear Structural Systems with Large Rigid Body Motion*, Pułtusk, Poland, July 2–7, 2000.

bodies has the advantage of using only one type of rigid-flexible joint, the rigid joint. Therefore, only the kinematic constraints for this type of joint must be derived and implemented in the flexible multibody code. For this kinematic joint one or more nodes of the flexible body are rigidly attached to the virtual body, constraining all its 6 degrees of freedom.

The virtual rigid bodies have null mass and inertia that can raise some numerical instability derived from ill conditioned and near singular system matrix. In order to minimize numerical problems a proper choice of integration algorithms and solvers of the system equations must be made. The equations of motion derived by using Cartesian and generalized flexible coordinates lead to very sparse matrix forms which are suitable to be solved by sparse matrix solvers [6, 7]. The use of such a method reduces the most of the computational burden derived from using virtual rigid bodies.

The application to complex mechanical systems lead to models with very large number of integration variables, associated with the flexible coordinates degrees of freedom. In order to achieve reasonable computer efficiency some nodal degrees of freedom reduction techniques must be used. In this work the component mode synthesis [16] is applied to describe the linear structural deformation of the flexible bodies. Boundary conditions consistent with the location of the floating frames are applied in the determination of the natural vibration modes and frequencies. The use of structural damping, as long as it level is kept small, has the advantage of improving the numerical efficiency of the numerical integrators without leading to major variations in the results [3].

The methodology proposed is applied to a flexible slider crank mechanism, which has been serving as a benchmark for many authors [12]. The results obtained are compared with those reported in others works in order to discuss the relative computational efficiency of the different methodologies, models and algorithms used.

In order to exploit the advantages of this methodology the dynamic analysis of a road vehicle, with a flexible chassis, is made. The computational costs associated with the use of virtual rigid bodies is compared to that of the use of the flexible bodies kinematic joints, specially derived and implemented in the multibody code. The results are discussed in terms of its numerical accuracy and efficiency.

2. Flexible multibody equations of motion

The description of the flexibility of multibody systems must have no dependency in the type of coordinates used to describe the body fixed coordinate systems. In this work the position of a body reference frame is defined by a set of Cartesian coordinates. The position and orientation of rigid body i is defined by a set of translation coordinates $\mathbf{r}_i = [x\ y\ z]^T$ and rotational coordinates described by Euler parameters $\mathbf{p}_i = [e_0\ e_1\ e_2\ e_3]^T$. To minimize the number of variables for integration, while improving the numerical stability of the computer implementation, the rigid body velocities and accelerations associated with the Euler parameters are transformed in angular velocities and accelerations [13]. The main advantage of the use of these coordinates is the simplicity of computational implementation of the equations of motion obtained.

2.1. Flexible body motion

Let it be assumed that a flexible body is composed of a coordinate system rigidly attached to a point on the flexible body, as depicted in Fig. 1. Let it also be assumed that the flexible body is represented using the finite element method, with lumped formulation for the mass matrix, and where the reference frame, described by vector $\mathbf{r}_i$ is located in the body center of mass.

Let the position of a node k of the flexible body be represented by

$$\mathbf{d}_k = \mathbf{r}_i + \mathbf{A}_i \mathbf{b}'_k \tag{1}$$

where $\mathbf{b}'_k = \mathbf{x}'_k + \boldsymbol{\delta}'_k$ is the position of node k in the body-fixed frame, being $\boldsymbol{\delta}'_k$ its deformation and $\mathbf{x}'_k$ the initial position, also measured in the local frame, and $\mathbf{A}_i$ is the transformation matrix

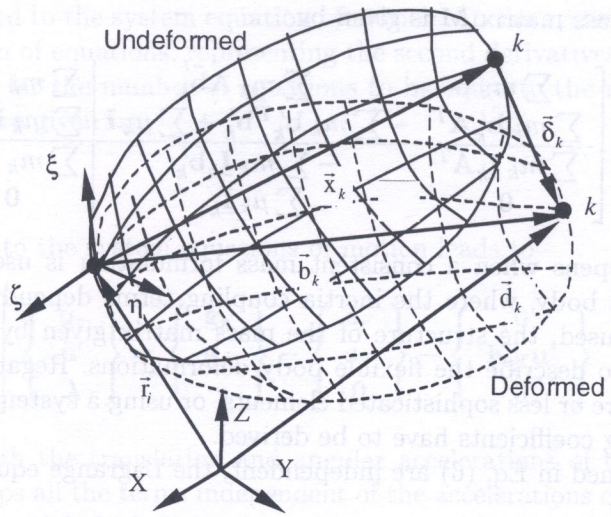

Fig. 1. Global position of node k

between the local and the inertial frames. Deriving the position equation with respect to time results in the node velocity, given by [1]

$$\dot{\mathbf{d}}_k = \dot{\mathbf{r}}_i + \mathbf{A}_i \tilde{\boldsymbol{\omega}}'_i \mathbf{b}'_k + \mathbf{A}_i \dot{\boldsymbol{\delta}}'_k \tag{2}$$

where $\boldsymbol{\omega}'_i$ is the angular velocity of the body fixed frame, expressed in the local frame. The evaluation of the kinetic energy involves the nodal angular velocity also. This is given by

$$\boldsymbol{\alpha}'_k = \boldsymbol{\omega}'_i + \dot{\boldsymbol{\theta}}'_k \tag{3}$$

where $\boldsymbol{\alpha}'_k$ is the generalized nodal angular velocity and $\dot{\boldsymbol{\theta}}'_k$ is the local nodal deformation velocity. The kinetic energy associated to node k with a mass m_k and a rotational inertia μ_k is

$$T_k = \frac{1}{2} m_k \, \dot{\mathbf{d}}^{k\,T} \dot{\mathbf{d}}^k + \frac{1}{2} \mu_k \, \boldsymbol{\alpha}'^{\,T}_k \boldsymbol{\alpha}'_k \,. \tag{4}$$

Finally, the kinetic energy of the complete flexible body is evaluated by summing the contribution of all n nodes

$$T = \frac{1}{2} \sum_{k=1}^{n} m_k \, \dot{\mathbf{d}}^{k\,T} \dot{\mathbf{d}}^k + \frac{1}{2} \sum_{k=1}^{n} \mu_k \, \boldsymbol{\alpha}'^{\,T}_k \boldsymbol{\alpha}'_k \,. \tag{5}$$

Before proceeding, let the coordinates used to describe the flexible body motion be represented by vector $\mathbf{q}_i$ containing coordinates associated to the motion of the body-fixed frame and the coordinates associated to the nodal displacements and rotations with respect to the local frame.

The velocity vector for the flexible body, represented by $\dot{\mathbf{q}}_i$ is written as

$$\dot{\mathbf{q}}_i = \left[\dot{\mathbf{r}}_i^T \; \boldsymbol{\omega}'^{\,T}_i \; \dot{\mathbf{u}}'^{\,T} \right]^T \tag{6}$$

where $\dot{\mathbf{u}}' = \left[\dot{\boldsymbol{\delta}}'^{\,T} \; \dot{\boldsymbol{\theta}}'^{\,T} \right]^T$ is the vector of the local nodal velocities.

The flexible body kinetic energy is now expressed in terms of the coordinates just defined. Substituting the definition given by Eq. (6) in Eq. (5) and rearranging leads to

$$T_i = \frac{1}{2} \dot{\mathbf{q}}_i^T \, \mathbf{M}_i \, \dot{\mathbf{q}}_i \tag{7}$$

where the flexible body mass matrix $\mathbf{M}$ is given by

$$\mathbf{M} = \begin{bmatrix} \mathbf{M}_r & \mathbf{M}_{rf} \\ \mathbf{M}_{fr} & \mathbf{M}_{ff} \end{bmatrix} = \left[\begin{array}{cc|cc} \sum m_k \mathbf{I} & -\sum m_k \mathbf{A}\tilde{\mathbf{b}}'_k & \sum m_k \mathbf{A}\underline{\mathbf{I}}_k^T & \mathbf{0} \\ \sum m_k \tilde{\mathbf{b}}'_k \mathbf{A}^T & -\sum m_k \tilde{\mathbf{b}}'^T_k \tilde{\mathbf{b}}'_k + \sum \mu_k \mathbf{I} & \sum m_k \tilde{\mathbf{b}}'_k \underline{\mathbf{I}}_k^T & \sum \mu_k \underline{\mathbf{I}}_k^T \\ \hline \sum m_k \underline{\mathbf{I}}_k \mathbf{A}^T & -\sum m_k \underline{\mathbf{I}}_k \tilde{\mathbf{b}}'_k & \sum m_k \underline{\mathbf{I}}_k \underline{\mathbf{I}}_k^T & \mathbf{0} \\ \mathbf{0} & \sum \mu_k \underline{\mathbf{I}}_k & \mathbf{0} & \sum \mu_k \underline{\mathbf{I}}_k \underline{\mathbf{I}}_k^T \end{array}\right] . \quad (8)$$

Contrary to what happens when a consistent mass formulation is used in the finite element description of the flexible body, where the inertia coupling terms depend on the particular finite element shape functions used, the structure of the mass matrix given by Eq. (8) is independent of the formulation used to describe the flexible body deformations. Regardless of using the finite element method, with more or less sophisticated elements, or using a system of springs and dampers no special inertia coupling coefficients have to be derived.

As all coordinates defined in Eq. (6) are independent, the Lagrange equations of motion for the flexible body are given by

$$\frac{\mathrm{d}}{\mathrm{d}t}\left(\frac{\partial T_i}{\partial \dot{\mathbf{q}}_i}\right) - \left(\frac{\partial T_i}{\partial \mathbf{q}_i}\right) + \left(\frac{\partial U_i}{\partial \mathbf{q}_i}\right) - \mathbf{g}_i = \mathbf{0} \quad (9)$$

where the elastic energy U_i is written in a generic form as

$$U_i = \frac{1}{2}\mathbf{q}_i^T \mathbf{K}_i \mathbf{q}_i \,. \quad (10)$$

Notice that the stiffness matrix $\mathbf{K}_i$ used in the equation for the elastic energy can be the finite element stiffness matrix or any other equivalent matrix, depending on the adopted description of the body flexibility. However, if matrix $\mathbf{K}_i$ is not dependent on the deformation of the flexible body it is implied in the formulation that only linear elastic deformations are assumed. That is the case for all that follows.

The definitions of the kinetic and elastic energy, given by Eqs. (7) and (10) respectively, are now substituted in Eq. (9) leading to

$$\mathbf{M}_i \ddot{\mathbf{q}}_i = \mathbf{g}_i + \mathbf{s}_i - \mathbf{K}_i \mathbf{q}_i \,. \quad (11)$$

In this equation $\mathbf{g}_i$ is the vector of external applied forces and vector $\mathbf{s}_i$ contains the quadratic velocity terms written here as

$$\mathbf{s} = \left\{ \begin{array}{c} -\sum m_k \mathbf{A}\tilde{\omega}'\tilde{\omega}'\mathbf{b}'_k - 2\sum m_k \mathbf{A}\tilde{\omega}'\dot{\delta}'_k \\ -\sum m_k \tilde{\mathbf{b}}'_k\tilde{\omega}'\tilde{\omega}'\mathbf{b}'_k - 2\sum m_k \tilde{\mathbf{b}}'_k\tilde{\omega}'\dot{\delta}'_k \\ -\sum m_k \underline{\mathbf{I}}_k\tilde{\omega}'\tilde{\omega}'\mathbf{b}'_k - 2\sum m_k \underline{\mathbf{I}}_k\tilde{\omega}'\mathbf{A}^T\dot{\delta}'_k \\ \mathbf{0} \end{array} \right\} . \quad (12)$$

A set of reference conditions is required to ensure uniqueness of the displacement field. For this purpose it is assumed here that a set of nodes of the flexible body is fixed to the body fixed coordinate system, i.e., the nodal displacements of these node with respect to the local frame are null. Other sets of reference conditions, such as the mean axis condition [14] can be used. The interested reader will find a discussion on this issue in references [14, 16, 17].

2.2. Flexible multibody system equation of motion

For a multibody system it is necessary to define a set of kinematic constraints describing the joints that restrict the relative motion between the system components. By using Lagrange multipliers this

set of constraints is added to the system equation of motion. To the system of equations obtained in this form another system of equations, representing the second derivatives the constraint equations, must be added in order for the number of equations to be equal to the number of unknowns. The acceleration equations are given by

$$\ddot{\mathbf{\Phi}} = \mathbf{\Phi}_{\mathbf{q}}\ddot{\mathbf{q}} - \boldsymbol{\gamma} = \mathbf{0}. \tag{13}$$

Adding these equations to the system equations of motion leads to

$$\begin{bmatrix} \mathbf{M}_r & \mathbf{M}_{rf} & \mathbf{\Phi}_{\mathbf{q}_r}^T \\ \mathbf{M}_{fr} & \mathbf{M}_{ff} & \mathbf{\Phi}_{\mathbf{q}_f}^T \\ \mathbf{\Phi}_{\mathbf{q}_r} & \mathbf{\Phi}_{\mathbf{q}_f} & \mathbf{0} \end{bmatrix} \begin{Bmatrix} \ddot{\mathbf{q}}_r \\ \ddot{\mathbf{u}}' \\ \boldsymbol{\lambda} \end{Bmatrix} = \begin{Bmatrix} \mathbf{g}_r \\ \mathbf{g}_f \\ \boldsymbol{\gamma} \end{Bmatrix} - \begin{Bmatrix} \mathbf{s}_r \\ \mathbf{s}_f \\ \mathbf{0} \end{Bmatrix} - \begin{Bmatrix} \mathbf{0} \\ \mathbf{K}_{ff}\mathbf{u}' \\ \mathbf{0} \end{Bmatrix} \tag{14}$$

where $\ddot{\mathbf{q}}_r$ is a vector with the translation and angular accelerations of the body fixed coordinate frame and vector $\boldsymbol{\gamma}$ groups all the terms independent of the accelerations coordinates. The system of equations (14) is a differential algebraic system of equations [9]. The DAE system are not ordinary differential equations but can be solved by using a ODE time integrator.

Note that the coupling between the rigid body motion and the system elastodynamics is fully preserved. If the finite element method is used to represent the flexibility of the system components all terms used in Eq. (14) are readily available from any commercial finite element package, regardless of the particular type of linear finite elements used in the model. The only restrictions, in the models obtained, are related with good finite element modeling practices. In particular, the use higher order finite elements should be avoided due to the lumped mass formulation, as they may lead to incorrect representation of the mass matrix.

2.3. Flexible coordinates reduction by component mode synthesis

The equations of motion for the flexible multibody systems, in the form described by Eq. (14), lead to a inefficient numerical implementation due to the large number of generalized coordinates necessary to describe complex models. This problem is overcome by using a component mode synthesis methodology. Though only the natural modes of vibration are used in this formulation other modes, such as the static correction modes [17], could also be considered in order to improve numerical precision and efficiency.

Let the nodal displacements of the flexible part of the body be described by a weighted sum of the modes of vibration associated with the flexible bodies lower natural frequencies,

$$\mathbf{u}' = \mathbf{X}\mathbf{w}, \tag{15}$$

where the vector $\mathbf{w}$ represents the contributions of the vibration modes towards the nodal displacements and $\mathbf{X}$ is the modal matrix. Note that, due to the reference conditions, the modes of vibration used in this formulation are constrained modes. Moreover, due to the assumption of linear elastic deformations the modal matrix is invariant. A simpler system of equations is obtained by the orthonormality of the modes of vibration with respect to the mass matrix implies that $\mathbf{X}^T\mathbf{M}_{ff}\mathbf{X} = \mathbf{I}$ and $\mathbf{X}^T\mathbf{K}_{ff}\mathbf{X} = \mathbf{\Lambda}$, where $\mathbf{\Lambda}$ is a diagonal matrix containing the squares of the flexible body natural frequencies. This leads to

$$\begin{bmatrix} \mathbf{M}_r & \mathbf{M}_{rf}\mathbf{X} & \mathbf{\Phi}_{\mathbf{q}_r}^T \\ \mathbf{X}^T\mathbf{M}_{fr} & \mathbf{I} & \mathbf{X}^T\mathbf{\Phi}_{\mathbf{q}_f}^T \\ \mathbf{\Phi}_{\mathbf{q}_r} & \mathbf{\Phi}_{\mathbf{q}_f}\mathbf{X} & \mathbf{0} \end{bmatrix} \begin{Bmatrix} \ddot{\mathbf{q}}_r \\ \ddot{\mathbf{w}} \\ \boldsymbol{\lambda} \end{Bmatrix} = \begin{Bmatrix} \mathbf{g}_r \\ \mathbf{X}^T\mathbf{g}_f \\ \boldsymbol{\gamma} \end{Bmatrix} - \begin{Bmatrix} \mathbf{s}_r \\ \mathbf{X}^T\mathbf{s}_f \\ \mathbf{0} \end{Bmatrix} - \begin{Bmatrix} \mathbf{0} \\ \mathbf{\Lambda}\mathbf{w} \\ \mathbf{0} \end{Bmatrix}. \tag{16}$$

All terms required for this equation, related with a finite element model, are obtained directly from commercial finite element codes.

3. Flexible bodies kinematic joints

For a multibody system different kinematic joints between the bodies must be defined. These joints may involve only rigid bodies, only flexible bodies or may involve a flexible and a rigid body. The spherical joints for these cases are shown here for the generalized elastic coordinates used in Eq. (14) or in Eq. (16), depending on the set of generalized elastic coordinates selected to represent the model.

3.1. Spherical joint between rigid bodies

The spherical joint between two rigid bodies is obtained by imposing that a common point in both bodies must have the same position every time. This is presented in Fig. 2.

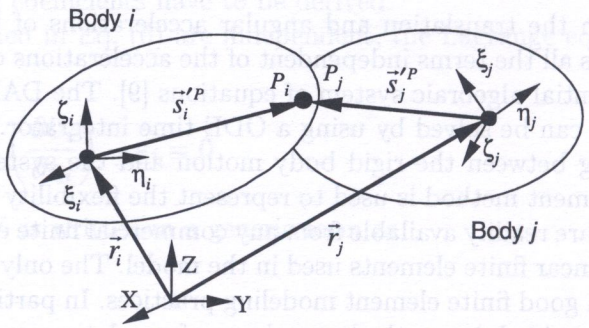

Fig. 2. Spherical joint between rigid body i and rigid body j

The constraint equations for the spherical joint between two bodies are

$$\mathbf{\Phi}_{\text{Sph}}^{(\text{rig}-\text{rig})} = \mathbf{r}_i^P - \mathbf{r}_j^P = \mathbf{0} \tag{17}$$

where $\mathbf{r}_i^P$ and $\mathbf{r}_j^P$ are global positions of the points in each body that are used to define the spherical joint. Expressing the points position as the global position of the body fixed frame plus the local position vector of each point, results in

$$\mathbf{\Phi}_{\text{Sph}}^{(\text{rig}-\text{rig})} = \mathbf{r}_i + \mathbf{A}_i\mathbf{s}_i'^P - \mathbf{r}_j - \mathbf{A}_j\mathbf{s}_j'^P = \mathbf{0}. \tag{18}$$

The constraint equation velocity is obtained as the first derivative in order to time of the constraint equation

$$\dot{\mathbf{\Phi}}_{\text{Sph}}^{(\text{rig}-\text{rig})} = \dot{\mathbf{r}}_i + \mathbf{A}_i\tilde{\boldsymbol{\omega}}_i'\mathbf{s}_i'^P - \dot{\mathbf{r}}_j - \mathbf{A}_j\tilde{\boldsymbol{\omega}}_j'\mathbf{s}_j'^P = \mathbf{0}. \tag{19}$$

The constraint equation acceleration is obtained by deriving two times in order to time, given

$$\ddot{\mathbf{\Phi}}_{\text{Sph}}^{(\text{rig}-\text{rig})} = \ddot{\mathbf{r}}_i + \mathbf{A}_i\tilde{\boldsymbol{\omega}}'\tilde{\boldsymbol{\omega}}_i'\mathbf{s}_i'^P + \mathbf{A}_i\dot{\tilde{\boldsymbol{\omega}}}'\mathbf{s}_i'^P - \ddot{\mathbf{r}}_j - \mathbf{A}_j\tilde{\boldsymbol{\omega}}_j'\tilde{\boldsymbol{\omega}}_j'\mathbf{s}_j'^P - \mathbf{A}_j\dot{\tilde{\boldsymbol{\omega}}}_j'\mathbf{s}_j'^P = \mathbf{0}. \tag{20}$$

This equation is rearranged in a matrix form as

$$\ddot{\mathbf{\Phi}}_{\text{Sph}}^{(\text{rig}-\text{rig})} = \mathbf{\Phi}_{\mathbf{q}}\ddot{\mathbf{q}} - \boldsymbol{\gamma} = \begin{bmatrix} \mathbf{I} & \mathbf{A}_i\mathbf{s}_i'^P & \mathbf{I} & \mathbf{A}_j\mathbf{s}_j'^P \end{bmatrix} \begin{bmatrix} \ddot{\mathbf{r}}_i \\ \boldsymbol{\omega}_i' \\ \ddot{\mathbf{r}}_j \\ \dot{\boldsymbol{\omega}}_j' \end{bmatrix} - \boldsymbol{\gamma} = \mathbf{0} \tag{21}$$

where vector $\boldsymbol{\gamma}$ groups all the terms independent of the accelerations coordinates.

3.2. Spherical joint between a flexible body and a rigid body

The kinematic joint between a flexible body and a rigid body is derived for a node k of the flexible body and a point P_j in the rigid body, as presented in Fig. 3. The kinematic constraints are obtained in order to ensure that the position of the node k and the point P_j are coincident at all time.

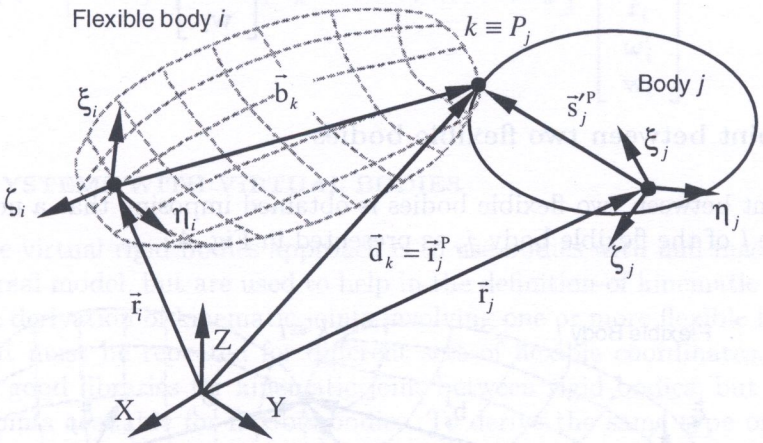

Fig. 3. Kinematic joint between flexible body i and a body j

The constraint equations for the spherical joint are

$$\mathbf{\Phi}^{(\text{flex-rig})}_{\text{Sph}} = \mathbf{r}^P_j - \mathbf{d}_k = \mathbf{0} \tag{22}$$

where $\mathbf{d}_k$ is the node position and the point P position given by $\mathbf{r}^P_j = \mathbf{r}_j + \mathbf{A}_j \mathbf{s}'^P_j$. Expressing the node position has in terms of Eq. (1) results in

$$\mathbf{\Phi}^{(\text{flex-rig})}_{\text{Sph}} = \mathbf{r}_j + \mathbf{A}_j \mathbf{s}'^P_j - \mathbf{r}_i - \mathbf{A}_i \mathbf{b}'_k = \mathbf{0}. \tag{23}$$

The nodal velocity of node k can be written in terms of the nodal translation and angular velocities given by $\dot{\boldsymbol{\delta}}'_k$ and $\dot{\boldsymbol{\theta}}'_k$, respectively. The constraint equation velocity is then

$$\dot{\mathbf{\Phi}}^{(\text{flex-rig})}_{\text{Sph}} = \dot{\mathbf{r}}_j - \mathbf{A}_j \tilde{\mathbf{s}}'^P_j \boldsymbol{\omega}'_j - \dot{\mathbf{r}}_i + \mathbf{A}_i \tilde{\mathbf{b}}'_k \boldsymbol{\omega}'_i - \mathbf{A}_i \dot{\boldsymbol{\delta}}'_k = \mathbf{0}. \tag{24}$$

Assembling the constraint equation in a matrix form, they are written as

$$\dot{\mathbf{\Phi}}^{(\text{flex-rig})}_{\text{Sph}} = \mathbf{\Phi}_{\mathbf{q}} \dot{\mathbf{q}} = \begin{bmatrix} \mathbf{I} & -\mathbf{A}_j \tilde{\mathbf{s}}'^P_j & -\mathbf{I} & \mathbf{A}_i \tilde{\mathbf{b}}'_k & \underline{\mathbf{A}}_i \end{bmatrix} \begin{bmatrix} \dot{\mathbf{r}}_j \\ \boldsymbol{\omega}'_j \\ \dot{\mathbf{r}}_i \\ \boldsymbol{\omega}'_i \\ \dot{\mathbf{u}}_i \end{bmatrix} = \mathbf{0} \tag{25}$$

where the $\underline{\mathbf{A}}_i$ matrix is a null matrix, except for the submatrix $\mathbf{A}_i$ that multiplies $\dot{\boldsymbol{\delta}}'_k$. If the modal degrees of freedom are used, as in Eq. (16), then $\dot{\boldsymbol{\delta}}'_k = \mathbf{X}^{\delta}_k \dot{\mathbf{w}}$. The matrix $\mathbf{X}^{\delta}_k$ is a submatrix of the modal matrix $\mathbf{X}$, associated to translations degrees of freedom of the node k. Replacing in the constraint equation results in

$$\dot{\mathbf{\Phi}}^{(\text{flex-rig})}_{\text{Sph}} = \dot{\mathbf{r}}_j - \mathbf{A}_j \tilde{\mathbf{s}}'^P_j \boldsymbol{\omega}'_j - \dot{\mathbf{r}}_i + \mathbf{A}_i \tilde{\mathbf{b}}'_k \boldsymbol{\omega}'_i - \mathbf{A}_i \mathbf{X}^{\delta}_k \dot{\mathbf{w}} = \mathbf{0}. \tag{26}$$

Assembling the constraint equation in a matrix form, for the modal degrees of freedom results in

$$\dot{\Phi}_{\text{Sph}}^{(\text{flex-rig})} = \Phi_{\mathbf{q}}\dot{\mathbf{q}} = \begin{bmatrix} \mathbf{I} & -\mathbf{A}_j\tilde{\mathbf{s}}_j'^{P} & -\mathbf{I} & \mathbf{A}_i\tilde{\mathbf{b}}_k' & \mathbf{A}_i\mathbf{X}_k^{\delta} \end{bmatrix} \begin{bmatrix} \dot{\mathbf{r}}_j \\ \boldsymbol{\omega}_j' \\ \dot{\mathbf{r}}_i \\ \boldsymbol{\omega}_i' \\ \dot{\mathbf{w}}_i \end{bmatrix} = \mathbf{0}. \tag{27}$$

3.3. Spherical joint between two flexible bodies

The kinematic joint between two flexible bodies is obtained imposing that a node k of the flexible body i and a node l of the flexible body j, as presented in Fig. 4.

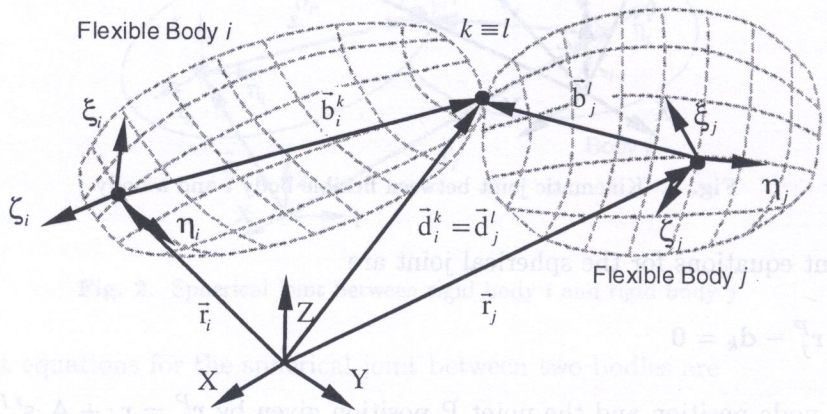

Fig. 4. Kinematic joint between two flexible bodies

The constraint equations for the spherical joint in this case are

$$\Phi_{\text{Sph}}^{(\text{flex-flex})} = \mathbf{d}_j^l - \mathbf{d}_i^k = \mathbf{0} \tag{28}$$

where each nodal position is given by Eq. (1). By substituting Eq. (1) in Eq. (28) the result is

$$\Phi_{\text{Sph}}^{(\text{flex-flex})} = \mathbf{r}_j + \mathbf{A}_j\mathbf{b}_j'^{l} - \mathbf{r}_i - \mathbf{A}_i\mathbf{b}_i'^{k} = \mathbf{0}. \tag{29}$$

The constraint equation velocity is then

$$\dot{\Phi}_{\text{Sph}}^{(\text{flex-flex})} = \dot{\mathbf{r}}_j + \mathbf{A}_j\tilde{\mathbf{b}}_j'^{l}\boldsymbol{\omega}_j' - \mathbf{A}_j\dot{\delta}_j'^{l} - \dot{\mathbf{r}}_i + \mathbf{A}_i\tilde{\mathbf{b}}_i'^{l}\boldsymbol{\omega}_i' - \mathbf{A}_i\dot{\delta}_i'^{k} = \mathbf{0}. \tag{30}$$

Assembling the constraint equation in a matrix form, this is written as

$$\dot{\Phi}_{\text{Sph}}^{(\text{flex-flex})} = \Phi_{\mathbf{q}}\dot{\mathbf{q}} = \begin{bmatrix} \mathbf{I} & \mathbf{A}_j\tilde{\mathbf{b}}_j'^{l} & -\underline{\mathbf{A}}_j & -\mathbf{I} & \mathbf{A}_i\tilde{\mathbf{b}}_i'^{k} & \underline{\mathbf{A}}_i \end{bmatrix} \begin{bmatrix} \dot{\mathbf{r}}_j \\ \boldsymbol{\omega}_j' \\ \dot{\mathbf{u}}_j \\ \dot{\mathbf{r}}_i \\ \boldsymbol{\omega}_i' \\ \dot{\mathbf{u}}_i \end{bmatrix} = \mathbf{0} \tag{31}$$

where matrices $\underline{\mathbf{A}}_i$ and $\underline{\mathbf{A}}_j$ have the same meaning described for Eq. (25). If the modal coordinates are used, the acceleration equations of the spherical joint becomes

$$\dot{\Phi}_{\text{Sph}}^{(\text{flex}-\text{flex})} = \Phi_{\mathbf{q}}\dot{\mathbf{q}} = \begin{bmatrix} \mathbf{I} & \mathbf{A}_j\tilde{\mathbf{b}}_j'^{l} & -\mathbf{A}_j\mathbf{X}_k^{\delta} & -\mathbf{I} & \mathbf{A}_i\tilde{\mathbf{b}}_i'^{k} & \mathbf{A}_i\mathbf{X}_k^{\delta} \end{bmatrix} \begin{bmatrix} \dot{\mathbf{r}}_j \\ \boldsymbol{\omega}_j' \\ \dot{\mathbf{w}}_j \\ \dot{\mathbf{r}}_i \\ \boldsymbol{\omega}_i' \\ \dot{\mathbf{w}}_i \end{bmatrix} = \mathbf{0}. \tag{32}$$

4. Multibody systems with virtual bodies

The idea behind the virtual rigid bodies approach is to use bodies with null mass and inertias that do not exist in the real model, but are used to help in the definition of kinematic joints that involve flexible bodies. The derivation of kinematic joints involving one or more flexible bodies, is generally a complex task that must be repeated for different sets of flexible coordinates. Most commercial codes have already good libraries for kinematic joint between rigid bodies, but are rather limited in the number of joints available for flexible bodies. To derive the same type of joints for flexible bodies is difficult and time consuming, and could lead to some numerical inefficiency if not done right. Table 1 summarizes some types of joints to be derived.

Table 1. Development of kinematic joints for flexible MBS

Standard Rigid Flexible MBS	*Virtual Bodies in Flexible MBS*
Rigid–Flexible Spherical Joint	Rigid Joint
Flexible–Flexible Spherical Joint	
Rigid–Flexible Revolute Joint	
Flexible–Flexible Revolute Joint	
Rigid–Flexible Cylindrical Joint	
Flexible–Flexible Cylindrical Joint	
Rigid–Flexible Prismatic Joint	
Flexible–Flexible Prismatic Joint	
Rigid–Flexible Universal Joint	
Flexible–Flexible Universal Joint	
Other (Special purpose joints)	

As shown before, the connection between rigid and flexible or between two flexible bodies requires a double effort in the joint derivation. The use of virtual bodies requires that only one type of joint for flexible bodies, is derived, i.e., the rigid joint. This is a joint that rigidly attaches one or more nodes of the flexible body to a rigid body. In the case of having only one node involved in the joint, this can be attached to the virtual body reference frame origin, leading to much simpler constraint equations. All joints already available can be used with flexible bodies by adding a virtual body for each flexible body connection point.

4.1. Flexible–rigid body rigid joint

The rigid joint between a flexible body and a virtual rigid body is derived for a node k of the flexible body and a point in the rigid body, coincident with the origin of the reference frame, as presented in Fig. 5. The kinematic joint is derived in order to constrain the relative translation and rotation of node k with respect to the rigid body reference frame. The number of such constraints is the same

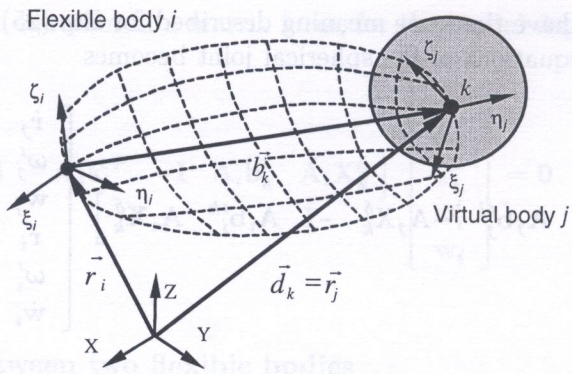

Fig. 5. Rigid joint between flexible body i and virtual body j

as the number of degrees of freedom introduced by the virtual rigid body. Therefore, the number of degrees of freedom of the system is the same as for a system without virtual bodies.

The constraint equations for the rigid joint are separated into translation and rotation constraints. The translation constraints are

$$\mathbf{\Phi}^{(t)} = \mathbf{r}_j - \mathbf{d}_k = \mathbf{0} \tag{33}$$

where $\mathbf{d}_k$ is the node position and $\mathbf{r}_j$ the virtual body reference frame position. Expressing the node position in terms of Eq. (1), results in

$$\mathbf{\Phi}^{(t)} = \mathbf{r}_j - \mathbf{r}_i - \mathbf{A}_i \mathbf{b}'_k = \mathbf{0}. \tag{34}$$

The nodal velocity of node k can be written in terms of the modal $\mathbf{X}_k^{\delta}$ and $\mathbf{X}_k^{\theta}$ submatricies of the modal matrix $\mathbf{X}$. The constraint equation velocity is then

$$\dot{\mathbf{\Phi}}^{(t)} = \dot{\mathbf{r}}_j - \dot{\mathbf{r}}_i + \mathbf{A}_i \tilde{\mathbf{b}}'_k \boldsymbol{\omega}'_i - \mathbf{A}_i \mathbf{X}_k^{\delta} \dot{\mathbf{w}} = \mathbf{0}. \tag{35}$$

To define the rotational constraint between a virtual body j and the node k of body i a procedure similar to that adopted by Shabana [15] is used. Let a nodal coordinate frame be attached to a node k. This nodal frame is defined by unit vectors $\mathbf{e}_k^l$ for $l = 1, 2, 3$ and is initially parallel to the body i fixed frame unit vectors $\mathbf{e}_i^l$. In the deformed configuration the global orientation of the nodal frame axes are written as

$$\hat{\mathbf{e}}_k^l = \mathbf{A}_i \mathbf{A}_i^k \mathbf{e}_k^l, \qquad \text{for} \qquad l = 1, 2, 3, \tag{36}$$

where $\mathbf{A}_i^k$ is the nodal rotation matrix for small rotations. The rotational constraint is imposed by enforcing that relative orientation between the axes of the virtual body j and the node k are invariant, i.e.

$$\mathbf{\Phi}^{(r)} = (\mathbf{A}_j \mathbf{e}_j^m)^T \mathbf{A}_i \mathbf{A}_i^k \mathbf{e}_k^l - \beta^{ml} = \mathbf{0} \qquad \text{for} \qquad l, m = 1, 2, 3, \tag{37}$$

where β^{ml} are constants and $\mathbf{e}_j^m$ are the unit vectors defined as $\mathbf{e}_j^1 = [1\ 0\ 0]^T$, $\mathbf{e}_j^2 = [0\ 1\ 0]^T$ and $\mathbf{e}_j^3 = [0\ 0\ 1]^T$. It should be noted that only three equations out of the nine equations implied in (37) are necessary to define the rotational constraint.

The time derivative of Eq. (37) yields the relation between angular velocities of bodies i and j and node k written as

$$\dot{\mathbf{\Phi}}^{(r)} = \boldsymbol{\omega}_j - \boldsymbol{\omega}_i - \mathbf{A}_i \mathbf{X}_k^{\theta} \dot{\mathbf{w}} \tag{38}$$

where the approximation $\mathbf{A}_i \mathbf{A}_i^k = \mathbf{A}_i$, which is valid for small deformations only, was used to simplify the equations. The constraint Eq. (38) is expressed in terms of local angular velocities as

$$\dot{\mathbf{\Phi}}^{(r)} = \mathbf{A}_i^T \mathbf{A}_j \boldsymbol{\omega}'_j - \boldsymbol{\omega}'_i - \mathbf{X}_k^{\theta} \dot{\mathbf{w}} = \mathbf{0}. \tag{39}$$

The Jacobian matrix is derived by arranging the expression in the form

$$\dot{\Phi} \equiv \Phi_q \dot{\mathbf{q}} = \mathbf{0}. \tag{40}$$

Assembling the velocity constraint equations for translation and rotations in a matrix form, leads to

$$\dot{\Phi} = \Phi_{\mathbf{q}} \dot{\mathbf{q}} = \begin{bmatrix} \mathbf{I} & \mathbf{0} & -\mathbf{I} & \mathbf{A}_i \tilde{\mathbf{b}}'_k & \mathbf{A}_i \mathbf{X}_k^{\delta} \\ \mathbf{0} & \mathbf{A}_i^T \mathbf{A}_j & \mathbf{0} & -\mathbf{I} & -\mathbf{X}_k^{\theta} \end{bmatrix} \begin{bmatrix} \dot{\mathbf{r}}_j \\ \boldsymbol{\omega}'_j \\ \dot{\mathbf{r}}_i \\ \boldsymbol{\omega}'_i \\ \dot{\mathbf{w}}_i \end{bmatrix} = \mathbf{0}. \tag{41}$$

Constraints acceleration equations are obtained by deriving Eq. (41) with respect to time, resulting in

$$\ddot{\Phi} = \Phi_{\mathbf{q}} \ddot{\mathbf{q}} - \gamma = \begin{bmatrix} \mathbf{I} & \mathbf{0} & -\mathbf{I} & \mathbf{A}_i \tilde{\mathbf{b}}'_k & \mathbf{A}_i \mathbf{X}_k^{\delta} \\ \mathbf{0} & \mathbf{A}_i^T \mathbf{A}_j & \mathbf{0} & -\mathbf{I} & -\mathbf{X}_k^{\theta} \end{bmatrix} \begin{bmatrix} \ddot{\mathbf{r}}_j \\ \dot{\boldsymbol{\omega}}'_j \\ \ddot{\mathbf{r}}_i \\ \dot{\boldsymbol{\omega}}'_i \\ \ddot{\mathbf{w}}_i \end{bmatrix} - \begin{bmatrix} \mathbf{A}_i \tilde{\boldsymbol{\omega}}'_i \left(\tilde{\boldsymbol{\omega}}'_i \mathbf{b}'_k - \mathbf{X}_k^{\delta} \dot{\mathbf{w}}_i \right) \\ \tilde{\boldsymbol{\omega}}'_i \mathbf{A}_i^T \mathbf{A}_j \boldsymbol{\omega}'_j \end{bmatrix} = \mathbf{0} \tag{42}$$

where vector γ groups all the terms independent of the accelerations coordinates.

4.2. Solution of the system equations of motion

The kinematic constraint are appended to the multibody system of equation of motion by using the Lagrange multipliers technique. For a flexible multibody system, where the component mode synthesis is used, the equations of motion are described by Eq. (16). The rigid body mass matrix $\mathbf{M}_r$ includes the contribution of all rigid bodies, and is null for the virtual rigid bodies.

The solution of the system equations of motion depicted by Eq. (16), using Cartesian coordinates, can represent 70 or 80% of the total computational time in a general multibody code analysis. A close look at the system equation matrix shows a large number of null elements and zero blocks with fixed size. The sparsity of the system matrix is very high and can be exploited in order to improve computational efficiency. The Gauss elimination scheme needed to solve the system of equations has a high number of arithmetic operations, proportional to the cube of the matrix dimension. With the use of a sparse matrix solver [6], the number of arithmetic operations is greatly reduced, becoming almost proportional to the number of nonzero elements in the system matrix. The use of a sparse matrix solver performs the Gauss elimination only on the non-zero elements of the matrix. In this work the Markowitz scheme with full pivot search is employed, reducing the number of fill-ins needed and showing good numerical stability [7]. The advantage of this scheme can be fully appreciated with the use of virtual rigid bodies, since only a few nonzero elements are appended to the system matrix. Therefore the computational cost of employing the virtual bodies method is greatly reduced.

4.3. Virtual bodies example: slider–crank mechanism

The virtual bodies methodology is applied and tested in a dynamic analysis of a slider crank mechanism with a flexible connecting rod. The mechanism data is presented in Table 2. This particular case has been extensively tested in the literature [12], having a good set of results published, which can be compared with those obtained by the methodology presented here.

Table 2. Slider crank data

Crank length	0.1524 m
Crank mass	10.0 kg
Crank angular velocity, ω	124.8 rad/s
Rod length	0.3048 m
Rod material	$E = 2.068{\cdot}10^{11}$ Pa; $\rho = 7820$ kg/m^3
Rod cross section	$3.16{\cdot}10^{-5}$ m^2
Slider mass	0.0 kg

The mechanism model has a flexible connecting rod, defined by a finite element structure with 8 beam elements. The crank and the slider are modelled as rigid bodies. To fully exploit the virtual bodies formulation, three cases are studied. In the first case two rigid bodies and a flexible body are used, and all the flexible-rigid kinematic joints are derived and implemented in the computer code. The two other cases use one and two virtual bodies, respectively, replacing the kinematic joints involving the flexible body by one rigid joint with the virtual body and one kinematic joint between the virtual and the rigid body. All models are presented in Fig. 6.

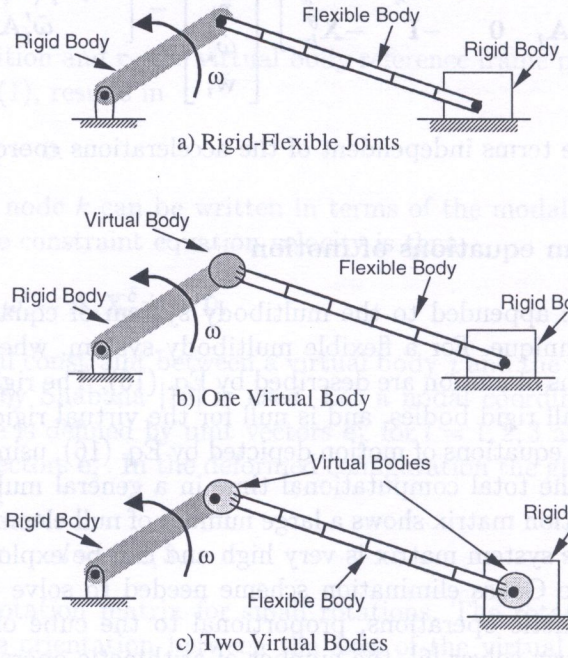

Fig. 6. Slider–crank models using virtual bodies

In order to study the sensitivity of method efficiency with respect to the increase in the number of bodies in the system, two algorithms are used. One that takes advantage of the sparse form of the system of equations while the other, uses a standard full matrix LU solver.

The numerical results obtained for the different simulations are presented in Fig. 7. The plot of a dimensionless parameter to quantify the mid rod deformation obtained by dividing the mid rod deformation by the rod length dimension is presented as a function of the simulation time.

The numerical efficiency for the different methodologies and algorithms is summarized by the results presented in Table 3. The computation time is normalized by dividing it by the time required to simulate the model without virtual bodies. The columns on the right show the time required for the system of equations solution.

The numerical results obtained show good agreement with the ones published in the literature [12], and almost no numerical differences are detected between the different models and al-

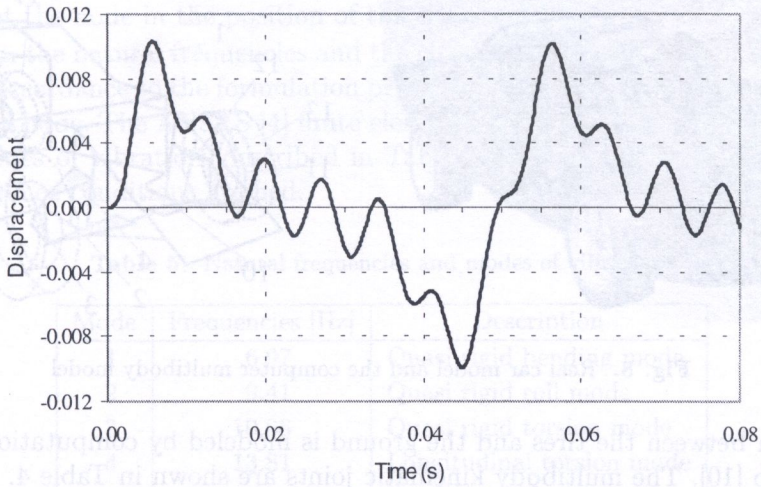

Fig. 7. Dimensionless parameter of mid rod deformation

Table 3. Numerical efficiency comparison

Bodies in the model	Analysis Time		System Equations Solution	
	Sparse	Full LU	Sparse	Full LU
Rigid (2), flexible (1)	1.00	1.19	1.00	1.17
Rigid (2), flexible (1), virtual (1)	1.08	1.86	1.03	1.50
Rigid (2), flexible (1), virtual (2)	1.33	2.40	1.14	2.04

gorithms. The use of a sparse matrix solver, which exploits the special sparsity of the system of equations matrix in the rigid-flexible multibody system, shows a clear advantage, particularly if virtual bodies are used. In such case, the numerical penalty due to the larger dimension of the system is not to so important. The use of virtual bodies presents, naturally, higher computational times, derived from the existence of more constraints equations and body coordinates in the model. The large number of variables for integration has also some negative influence in the integration algorithm, reducing the time step size and increasing the number of system evaluations required, which results in an even higher analysis time. An extra instability is introduced in the system by having a null mass and inertia for the virtual bodies originating an ill conditioned matrix. The use of iterative refinement in the solution methods is introduced to minimize the numerical errors arising from this type of problem.

5. Sports car dynamics using virtual bodies

The virtual bodies methodology applied to complex flexible multibody systems is exemplified by the numerical simulation of the dynamics of a sports car. The sports car is a replica of the Lancia Stratos, and was built in-house at IDMEC/IST. All the components mechanical characteristics and vehicle dimensions were obtained.

5.1. Multibody model of the sports car

The multibody model of the vehicle [2] is made of 17 bodies and 20 kinematics joints. The system components comprise the front suspension double arm, the rear McPherson suspension, the wheels and the chassis as shown in Fig. 8.

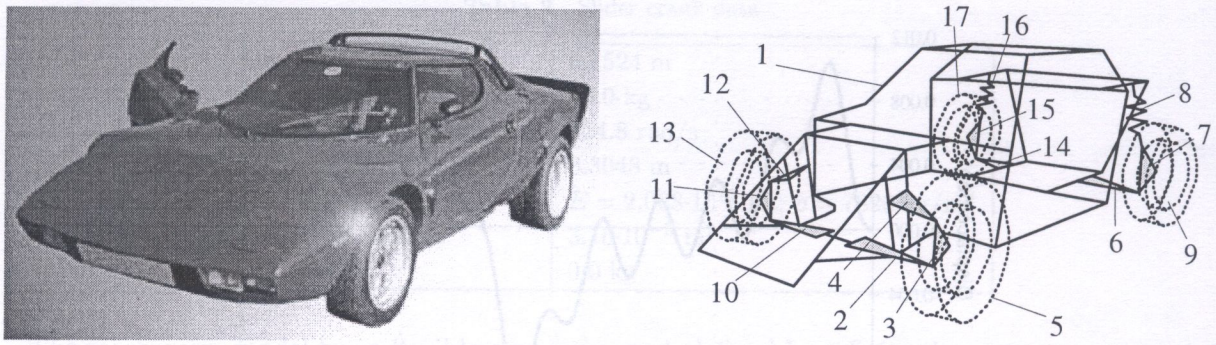

Fig. 8. Real car model and the computer multibody model

The interaction between the tires and the ground is modeled by computational tire model with comprehensive slip [10]. The multibody kinematic joints are shown in Table 4.

For the chassis body two different models are used. In the first one the chassis is modeled has a rigid body, and in the second one has a flexible body defined by a finite element structure. The vehicle shell is not used since it has a very small influence in the structural dynamics of the vehicle. For the flexible chassis model the kinematic joints have to be defined between a rigid and a flexible body. These joints need some special care and are referenced in Table 4 in italics.

The ANSYS [4] finite element code is used for the chassis structural model, shown in Fig. 9. The model has 282 nodes, representing 1680 degrees of freedom. Several type of finite elements are used,

Table 4. Kinematic joints data (in italics – the special joints between flexible and rigid bodies)

Joint	Type	Body i	Body j	Joint	Type	Body i	Body j
1	*Revolute*	*1*	*2*	11	Translation	8	7
2	*Revolute*	*1*	*4*	12	Revolute	7	9
3	Spherical	4	3	*13*	*Revolute*	*1*	*14*
4	Revolute	3	5	*14*	*Revolute*	*1*	*16*
5	*Revolute*	*1*	*10*	15	Translation	16	15
6	*Revolute*	*1*	*12*	16	Revolute	15	17
7	Spherical	11	12	17	Spherical	2	3
8	Revolute	11	13	18	Spherical	10	11
9	*Revolute*	*1*	*8*	19	Spherical	6	7
10	*Revolute*	*1*	*6*	20	Spherical	14	15

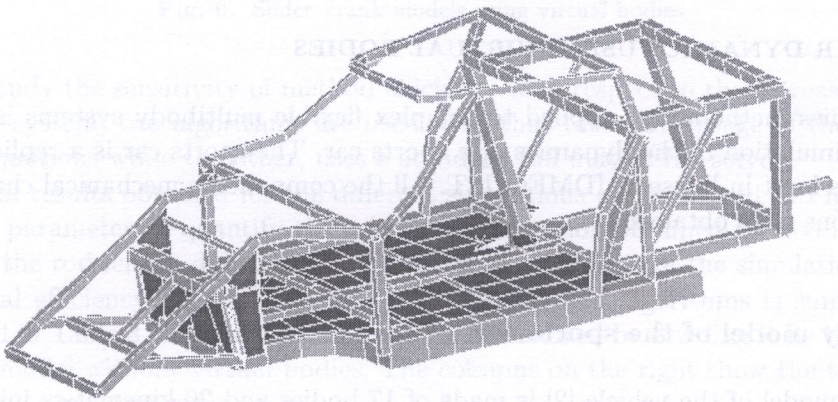

Fig. 9. Finite element model of the chassis

including 262 3D beams, 121 shell elements and 18 point mass elements. The origin of the local reference frame is at the node in the position of the chassis centre of mass.

In order to obtain the natural frequencies and the chassis modes of vibration reference conditions must be applied in accordance to the formulation presented. The node in the reference frame origin is considered as a fixed node. The ANSYS [4] finite element code is used to obtain the ten first natural frequencies and modes of vibration, described in Table 5. As an example, mode 4 is presented in Fig. 10 for the reference conditions applied.

Table 5. Natural frequencies and modes of vibration

Mode	Frequencies [Hz]	Description
1	6.97	Quasi rigid bending mode
2	9.41	Quasi rigid roll mode
3	10.96	Quasi rigid torsion mode
4	13.81	Longitudinal torsion mode
5	25.26	Bending mode
6	32.41	Vertical torsion mode
7	38.55	Bending and torsion mode
8	45.95	Lateral torsion mode
9	50.27	Local mode (floor plan)
10	50.31	Local mode (floor plan)

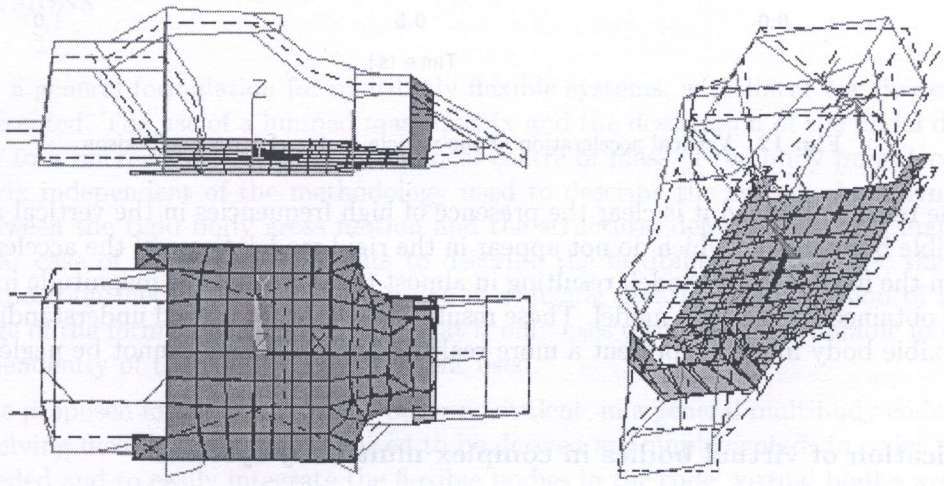

Fig. 10. Longitudinal torsion mode ($\omega_4 = 13.81$ Hz)

5.2. Dynamic simulation of riding over a road bump

The multibody model is used in a simulation of the vehicle riding over a road bump, with 10 cm of height, with the wheels of the left side, as shown in Fig. 11. The vehicle initial speed is of 60 km/h.

This simulation permits an evaluation of the vehicle behavior, stability and to study the influence of the chassis flexibility. Two simulations where carried out, one with a rigid body as chassis and the second one with a flexible body as chassis. From the numerical results, the vertical acceleration of the vehicle center of mass is chosen to show the differences between the two kinds of models. Figure 12 presents a plot of the accelerations.

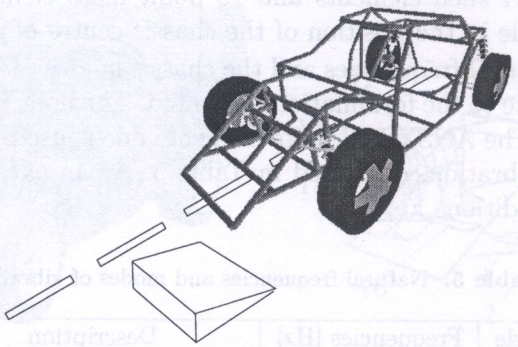

Fig. 11. Vehicle riding over a bump at 60 km/h

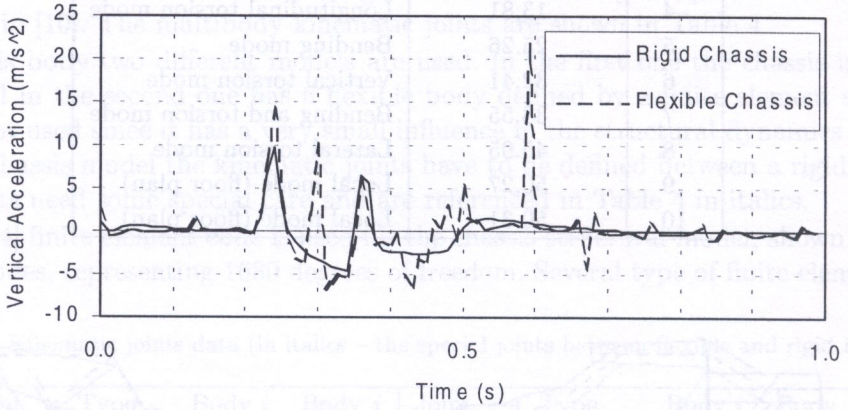

Fig. 12. Vertical acceleration of the vehicle centre of mass comparison

From the results obtained it is clear the presence of high frequencies in the vertical accelerations for the flexible body model, which do not appear in the rigid model. Some of the acceleration values are larger in the flexible body model, resulting in almost the double of the magnitude in comparison to the ones obtained by the rigid model. These results show that for a good understanding of vehicle ride the flexible body models represent a more realistic approach that cannot be neglected.

5.3. Application of virtual bodies in complex multibody systems

In the computer code developed for the multibody analysis with rigid and flexible bodies, two types of kinematic joints involving flexible bodies were derived. The spherical joint and the rigid joint. For the computer simulation of the vehicle two modelling possibilities are used, without the need to derive more kinematic joints between rigid and flexible bodies. In the first model two spherical rigid-flexible joints replace every revolute joint between a rigid and a flexible body. These joints are defined between the vehicle chassis and the suspension components. The second option is the use of virtual bodies. In this approach for every joint, between a rigid and a flexible body, one virtual body is added. In this way only revolute joints between rigid and virtual bodies and the rigid joint between virtual and flexible bodies are used. Each virtual body, added to the system, is attached to a node of the flexible chassis located in the joint position.

To evaluate the numerical efficiency a comparison between the analysis times is made for the different type of models used. Table 6 shows a summary of the analysis time efficiency by presenting the time ratio to the fastest analysis time of all models. Also the difference of using different types of methods for the resolution of the system of equations is represented. The numerical integration

scheme used, which is a variable time step method [8], shows some sensitivity to the average size of the time steps needed for the different models and methodologies.

Table 6. Analysis time comparison

Bodies in the model	System of Eq. Dimension	Analysis Efficiency	
		Sparse	Full LU
Rigid (17)	194	1.00	–
Rigid (16), flexible (1)	196	1.39	6.23
Rigid (16), flexible (1), virtual (8)	290	1.85	13.6

From the analysis time required for each type of model it is clear the advantage of using a sparse matrix solver, mainly for complex problems with a large number of bodies and larger system dimensions. In the case of using virtual bodies, the advantage is even higher. When other than sparse matrix solvers are used the computational overhead of such a methods is to heavy, resulting in analysis times that are one order of magnitude higher than for the initial model. The numerical results obtained show no difference on the results when different models and methodologies are applied.

6. Conclusions

In this work a general formulation for multibody flexible systems, with linear elastic deformations, has been presented. The use of a lumped mass matrix and the description of the nodal deformation with respect to a reference frame fixed in the local centre of mass of the body permitted to obtain a mass matrix independent of the methodology used to describe the system elastodynamics. The coupling between the rigid body gross motion and the structural deformations was maintained. In the particular case of using finite elements to describe the flexibility of the body, the use of the modal superposition method had the advantage of reducing greatly the dimension of the system. An advantage of the formulation presented is that it only uses terms readily available in commercial codes, independently of the type of finite element used.

To use the proposed formulation, or any other equivalent, in a general multibody code, new types of joints involving flexible bodies are required to be derived and implemented. In order to minimize the work needed and to easily integrate the flexible bodies in the code, virtual bodies are used. The virtual bodies are applied in the definition of the joints that involve flexible bodies, and required only for a rigid joint to be derived. The rigid joint is defined by fixing one or more nodes of the flexible body to the virtual body.

The addition of virtual bodies to the system has the numerical disadvantage of increasing the number of variables and constraints in the system. To minimize the impact of such methodology, a sparse matrix solver is applied resulting in a large decrease of the computational cost of using virtual bodies. The methodology is tested by simulating a flexible slider-crank mechanism and comparing the results with those published in the literature. The method is also applied to a complex system of a vehicle for its dynamic analysis. The vehicle is modelled using a flexible chassis and results are compared between a rigid chassis model and a flexible chassis model. The results clearly show the advantage of having a flexible chassis model, with the ability to give a more precise response of the vehicle dynamics characteristics and performance. Also for the complex model, the use of virtual bodies does not increase prohibitively the computational costs, provided that sparse matrix solvers are used.

Acknowledgments

This work was supported by Fundação para a Ciência e Tecnologia, by project PRAXIS 2/2.1/TPAR/2041/95 about "Métodos Avançados de Projecto e Concepção de Estruturas de Veículos em Condições de Serviço e Impacto" (Advanced Design Methods for Vehicle Structures Undergoing Impact and Service Conditions and the scholarship BD/9245/96.

References

[1] J. Ambrósio, J. Gonçalves. Complex flexible multibody systems with application to vehicle dynamics. In: J. Ambrósio, W. Schiehlen, eds., *Euromech Colloquium 404 - Advances in Computational Multibody Dynamics*, 241–258. IDMEC/IST, 1999.

[2] J. Ambrósio, J. Gonçalves. Complex flexible multibody systems with application to vehicle dynamics. *Multibody Systems Dynamics*, **6**(2): 163–182, 2001.

[3] J. Ambrósio, P. Ravn. Elastodynamics of multibody systems using generalized inertial coordinates and structural damping. *Mech. Struct. and Mach.*, **25**(2): 201–219, 1997.

[4] *ANSYS - Version 5.2.* Swanson Analysis Inc., 1995.

[5] D. Bae, J. Han, J. Choi. An implementation method for constrained flexible multibody dynamics using virtual body and joint. *Multibody Systems Dynamics*, **4**: 207–226, 2000.

[6] K. Crowe, J. Yuan-An, D. Neaderhouser, P. Smith. *A Direct Sparse Linear Equation Solver using Linked List Storage.* IMSL Technical Report 9006, IMSL, Houston, 1990.

[7] I. Duff, A. Erisman, J. Reid. *Direct Methods for Sparse Matrices.* Clarendon Press, Oxford, 1986.

[8] G. Gear. Numerical simulation of differential-algebraic equations. *IEE Translations on Circuit Theory*, **CT-18**: 89–95, 1981.

[9] C. Gear, L. Petzold. Ode methods for the solution of differential/algebraic systems. *SIAM J. Numer. Anal.*, **21**: 367–384, 1984.

[10] G. Gim, P. Nikravesh. An analytical model of pneumatic tire for vehicle dynamic simulations, Part I. *Int. J. of Vehicle Design*, **11**(6): 589–618, 1991.

[11] J. Gonçalves, J. Ambrósio. *Sistemas Mecânicos Rigido-Flexiveis Utilizando Coordenadas Naturais Para a Análise Dinâmica de Veículos* (Rigid-Flexible Mechanical Systems With Natural Coordinates For Vehicle Dynamics). Technical Report IDMEC 96/006, Institute of Mechanical Engineering, I.S.T., Portugal, 1996.

[12] J. Meijaard. Validation of flexible beam elements in dynamics programs. *Nonlinear Dynamics*, **9**: 21–36, 1996.

[13] P. Nikravesh. *Computer-Aided Analysis of Mechanical Systems.* Prentice Hall, New Jersey, 1988.

[14] M. Pereira, P. Proença. Dynamic analysis of spatial flexible multibody systems using joint coordinates. *Int. J. Num. Meth. Engng.*, **32**: 1799–1812, 1991.

[15] A. Shabana. *Dynamic Analysis of Large Scale Inertia Variant Flexible Mechanisms.* Ph.D. Thesis, University of Iowa, 1982.

[16] A. Shabana, R. Wehage. A coordinate reduction technique for transient analysis of spatial structures with large angular rotations. *Journal of Structural Mechanics*, **11**(3): 401–431, 1983.

[17] W. Yoo, E. Haug. Dynamics of flexible mechanical systems using vibration and static correction modes. *Journal of Mechanisms, Transmissions and Automation in Design*, **108**: 315–322, 1986.